COMPEL—The International Journal for Computation and Mathematics in Electrical and Electronic Engineering
Vol. 7, Nos. 1 & 2, 29–45 © 1988 BOOLE PRESS LIMITED

INFINITE CYLINDER IN A UNIFORM SINUSOIDAL FIELD (COMPARISON OF RESULTS, PROBLEM 2)

Nathan IDA
Electrical Engineering Department, The University of Akron, Akron, OH 44325, U.S.A.

ABSTRACT: Problem 2 of the International Workshop for Eddy Current Code Comparison is a hollow cylinder with its axis perpendicular to a uniform sinuosoidal field. A total of 10 solutions, employing 9 different computer codes, are described and compared with analytic results. Most codes were 2-D finite element and were found to give satisfactory solutions.

1. INTRODUCTION

The results reported here are a compilation of data presented at the Electromagnetic Workshop at Rutherford Appleton Laboratory in March 1986, at the Workshop at Argonne National Laboratory in June 1986 and at the International Workshop at Graz, Austria, in August 1987. A total of ten solutions to problem No. 2 are presented and compared directly in tables. In some cases, variations on the specified problem were also available. These are marked in the tables and the conditions under which the calculations were performed are explained.

Some of the results presented were not available in a form which allowed direct comparison. For example, the field values from PROFI were presented as radial and azimuthal components. These were included with the other results (x and y components) but any comparison should be made in the right context. In addition, not all field and phase angle data were available at all requested points.

In some cases, results for the problem were reported for more than one type of element, for different numbers of elements or for different boundaries. These are also marked in the tables.

2. PROBLEM DESCRIPTION

The problem solved here consists of an infinitely long cylinder with inner radius of 0.05715 m and outer radius of 0.06985 m. The cylinder is made of aluminum alloy 6061 with resistivity $=3.94 \times 10^{-08}$ Ωm. The cylinder and its dimensions are shown in Fig. 1. A uniform field of 0.1 Tesla at 60 Hz is applied perpendicular to the cylinder axis. In order to facilitate comparison, a mesh was recommended as shown in Fig. 2. The mesh has nodes at 0.01 m spacing in the region $0 \leqslant x \leqslant 0.03$, $0 \leqslant y \leqslant 0.03$ m. In the regions surrounding this square, the nodes on the inner radius of 0.05715 m are spaced 15° apart. The nodes on the other three boundaries have

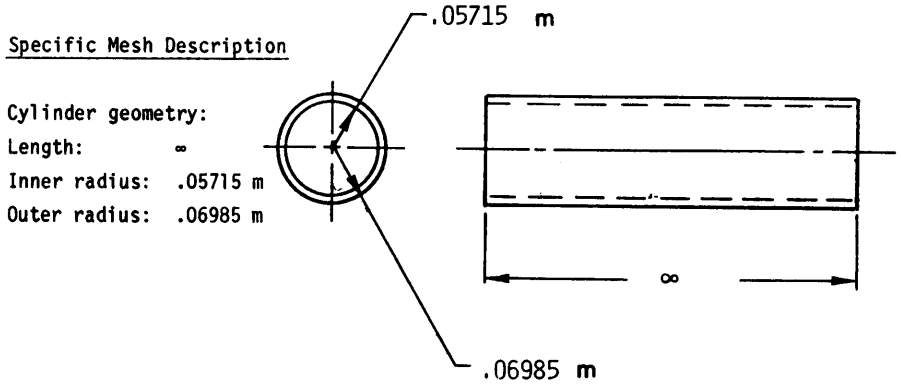

Figure 1: Cylinder geometry and dimensions.

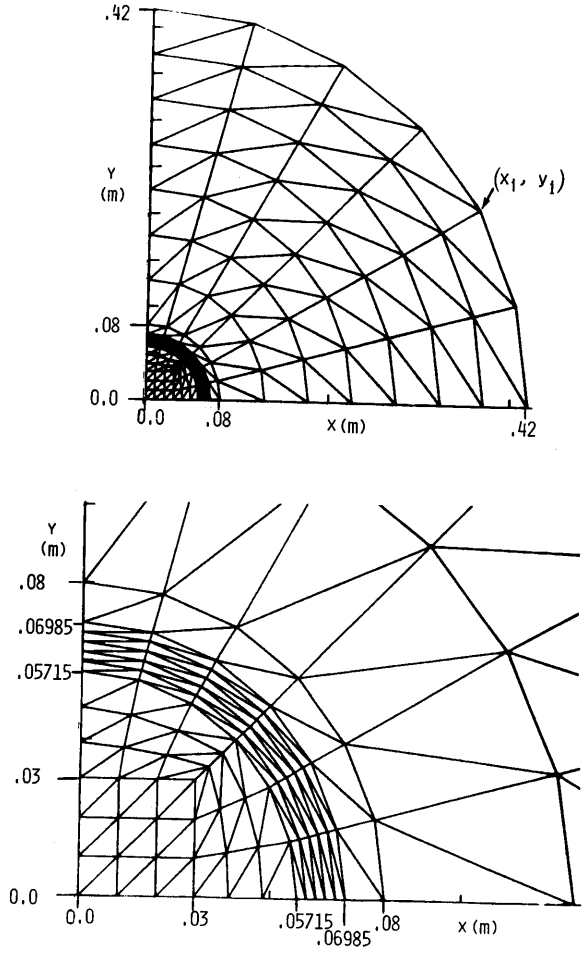

Figure 2: Specified mesh. (a) Whole mesh; (b) Detail at center of mesh.

equidistant spacing. Straight lines are drawn connecting the nodes on $y = 0.03$ (or $x = 0.03$) to the nodes on $r = 0.05715$. These lines have nodes equidistantly spaced. In the cylindrical region, nodes are placed at $r = 0.05715$, 0.05969, 0.06223, 0.06447, 0.06731, 0.06985 and 0.080 m and at $\theta = 0$, 15, 30, 45, 60, 75, and 90°. The total number of nodes is 128 and the number of (quadrilateral) elements is 105. The user was free to use other meshes in addition to this recommended mesh. A complete description of the problem can be found elsewhere [1, 2]. Other general information relevant to this work can be found in [3, 4].

2.1 Boundary Conditions

Boundary conditions were specified to create a Y-directed field of 0.1 T. The actual method of specification of boundary conditions was left open because different codes handle boundary conditions differently.

3. METHODS AND FORMULATIONS

Contributions to this summary were produced by 10 authors or groups of authors using 9 computer codes. Because these solutions are two-dimensional (2-D), the formulations and codes are quite similar. A short description of each follows. The letter in front of each name or code is later used for identification of results. When possible, references are also given.

(A) '*PE2D*' *C.R.I. Emson, Rutherford Appleton Laboratory*. A finite element formulation of the time harmonic Poisson's equation in cylindrical coordinates (Axisymmetric/2-D) is used for the solution.

$$\nabla \cdot (\nu \nabla A) = -j\omega\sigma A \tag{1}$$

Quadratic triangular elements and an ICCG algorithm were used for the results presented [5].

(B) '*PE2D*' *R.J. Lari and L. Turner, Argonne National Laboratory*. Program PE2D was used with either linear or quadratic triangular elements [6, 7] solving eq. (1).

(C) '*PROFI*' *U. Hamm, Technische Hochschule, Darmstadt*. Eq. (1) is solved in cylindrical coordinates using a finite difference formulation [8].

(D) '*No Name*' *T. Morisue, University of Tokushima*. A finite element formulation of eq. (1) with triangular (linear) elements is used [9].

(E) '*EDDYNDT*' *N. Ida, The University of Akron*. Eq. (1) is solved using linear quadrilateral elements and an ICCG solution algorithm [10].

(AN) '*Analytic*' *A. Ivanyi, I. Bardi and O. Biro, Technical University of Budapest*. The solution to the problem is found by solving the z-directed magnetic vector potential. This satisfies Laplace's equation in the air regions and Helmholtz' equation in the conductor. In cylindrical coordinates the solutions can be written by separation of variables. The azymuthal variation is harmonic and the radial is described in terms of power functions for Laplace's equation and of Bessel functions of the first kind for Helmholtz' equation. This solution was used for comparison of the various solutions [11].

(G) '*ANSYS*' *D.F. Ostergaard, Swanson Analysis Systems, Inc.* ANSYS uses a finite element formulation of eq. (1) in cylindrical coordinates [12, 13], with four node isoparametric elements and a frontal solver.

(H) '*No Name*' *E.M. Deeley, King's College.* A surface impedance formulation with the magnetic scalar potential as the variable is used, with linear triangular elements and an ICCG solver [14, 15].

(I) '*FIELD/A2JW*' *T. Nakata, N. Takahashi, K. Fujiwara and K. Okazaki, Okayama University.* Eq. (1) is solved with first order triangular elements and a Gauss Elimination algorithm [16].

(J) '*WEMAP*' *V.K. Garg, M. Ashkin and D. Simmen, Westinghouse Electric Corporation.* An axisymmetric formulation of eq. (1) with linear triangular elements is used [17].

4. RESULTS AND DISCUSSION

The results available for this problem are extensive. It is not possible to include all of them here; therefore only some representative results are summarized in Tables 1–4. The data in these tables were chosen to display the largest variations in results. For this reason, flux densities at most points inside and outside the cylinder were excluded with the exception of Table 1. In this table, the results inside the cylinder

Table 1
Field points on the X axis

R [m]	ϕ [Deg]	B_x [T]	θ_x [Deg]	B_y [T]	θ_y [Deg]	PROG.
0.0	0.0	0.0	0.0	0.0211	−95.0	AN
		0.0	−155.5	0.0220	−85.5	B2
		0.0	180.0	0.0206	−85.4	B3
		—	—	—	—	C
		0.0	0.0	0.0212	−95.0	D
		—	—	—	—	E
		0.0	0.0	0.0223	−94.4	G
		0.0	0.0	0.0218	−94.6	G1
		0.0	0.0	0.0214	−94.9	G2
		0.0000	—	0.0200	−82.8	H
		0.0	−178.3	0.0230	86.3	I
		0.0	179.6	0.0221	85.7	I1
		0.0	0.0	0.0218	85.6	J
0.01	0.0	0.0	0.0	0.0211	−95.0	AN
		0.0	−30.7	0.0233	−86.4	A
		0.00	−169.8	0.0229	−86.3	B
		0.0	93.8	0.0197	−85.6	B1
		0.0	−169.5	0.0220	−85.6	B2
		0.0	88.1	0.0206	−85.4	B3
		0.0001	−95.0	0.0220	−94.9	C
		0.0	—	0.0212	−95.0	D
		0.0	—	0.0275	−91.0	E
		0.0	—	0.0199	−82.8	H
		0.0	−178.4	0.0230	86.4	I
		0.0	179.3	0.0221	85.7	I1
		0.0	36.8	0.0218	85.6	J

Table 1 (*continued*)

R [m]	ϕ [Deg]	B_x [T]	θ_x [Deg]	B_y[T]	θ_y [Deg]	PROG.
0.02	0.0	0.0	0.0	0.0211	−95.0	AN
		0.0	−11.9	0.0233	−86.3	A
		0.0001	−175.5	0.0229	−86.4	B
		0.0	−41.5	0.0197	−85.6	B1
		0.0	−172.6	0.0220	−85.6	B2
		0.0	91.4	0.0206	−85.4	B3
		0.0002	−94.0	0.0220	−94.8	C
		0.0	—	0.0212	−95.0	D
		0.0008	—	0.0276	−91.0	E
		0.0	—	0.0198	−82.7	H
		0.0001	−178.2	0.0230	86.6	I
		0.0	179.0	0.0221	85.7	I1
		0.0	22.4	0.0218	85.6	J
0.03	0.0	0.0	0.0	0.0211	−95.0	AN
		0.0002	−4.7	0.0233	−86.0	A
		0.0002	−179.4	0.0230	−86.8	B
		0.0	174.0	0.0197	−85.6	B1
		0.0	−175.6	0.0220	−85.7	B2
		0.0	81.6	0.0206	−85.4	B3
		0.0002	−93.9	0.0220	−94.8	C
		0.0	—	0.0212	−95.0	D
		0.0008	—	0.0276	−91.0	E
		0.0	—	0.0196	−82.6	H
		0.0002	−177.6	0.0230	86.9	I
		0.0	179.4	0.0220	85.8	I1
		0.0	61.9	0.0218	85.6	J
0.04	0.0	0.0	0.0	0.0211	−95.0	AN
		0.0006	−3.4	0.0234	−85.0	A
		0.0006	178.1	0.0229	−87.7	B
		0.0	−178.9	0.0197	−85.6	B1
		0.0001	179.5	0.0220	−85.9	B2
		0.0	−109.7	0.0206	−85.4	B3
		0.002	−93.8	0.0220	−94.8	C
		0.0	—	0.0212	−95.0	D
		0.0008	−46.4	0.0276	−91.0	E
		0.0	—	0.0196	−82.5	H
		0.0005	−176.6	0.0229	87.7	I
		0.0001	−179.3	0.0220	86.0	I1
		0.0	15.0	0.0218	85.6	J
0.05	0.0	0.0	0.0	0.0211	−95.0	AN
		0.0017	−1.1	0.0235	−89.9	A
		0.0010	175.6	0.0230	−93.5	B
		0.0	−178.6	0.0197	−86.8	B1
		0.0004	178.4	0.0219	−86.8	B2
		0.0	−176.7	0.0206	−85.3	B3
		0.0002	−93.9	0.0220	−94.8	C
		0.0	—	0.0210	−95.0	D
		0.0008	−46.6	0.0275	−90.8	E
		0.0	—	0.0197	−82.4	H
		0.0010	−174.8	0.0212	93.7	I
		0.0004	−178.1	0.0219	86.8	I1
		0.0	−0.1	0.0218	85.9	J

Table 1 (*continued*)

R [m]	ϕ [Deg]	B_x [T]	θ_x [Deg]	B_y [T]	θ_y [Deg]	PROG.
0.05842	0.0	0.0	0.0	0.0280	−53.8	AN
		0.0052	−0.1	0.0363	−136.9	A
		0.0013	3.0	0.0293	−123.9	B
		0.0013	167.3	0.0287	−129.6	B1
		0.0003	28.8	0.0282	−125.7	B2
		0.0001	170.0	0.0278	−127.8	B3
		0.0002	−92.9	0.0290	−56.6	C
		0.0	0.0	0.0222	−35.8	D
		0.0009	−22.8	0.0295	−33.8	E
		0.0030	177.2	0.0320	−46.9	G
		0.0012	175.9	0.0288	−53.4	G1
		0.0012	175.6	0.0282	−53.6	G2
		0.0001	—	0.0260	−125.1	H
		0.0009	−13.4	0.0232	148.9	I
		0.0002	−38.5	0.0192	141.9	I1
		0.0023	2.7	0.0309	−48.4	J
0.06858	0.0	0.0	0.0	0.1667	2.1	AN
		0.0205	−11.4	0.1736	176.4	A
		0.0211	−10.2	0.1648	177.8	B
		0.0037	−22.7	0.1549	176.9	B1
		0.0110	−9.6	0.1710	177.6	B2
		0.0007	−23.6	0.1630	177.5	B3
		0.0002	−57.8	0.1710	2.3	C
		0.0	0.0	0.1630	−4.0	D
		0.0010	−10.4	0.1740	−3.3	E
		0.0196	−169.7	0.1619	2.1	G
		0.0106	−169.6	0.1711	2.7	G1
		0.0104	−169.9	0.1679	2.4	G2
		0.0	—	0.1568	178.8	H
		0.0205	9.7	0.1536	−173.2	I
		0.0109	9.4	0.1603	−171.4	I1
		0.0038	20.2	0.1728	3.1	J
0.075	0.0	0.0	0.0	0.1745	5.7	AN
		0.0184	−13.6	0.1708	174.5	A
		0.0205	−13.4	0.1690	174.9	B
		0.0028	−27.3	0.1600	174.1	B1
		0.0110	−14.0	0.1801	173.8	B2
		0.0001	−167.7	0.1697	174.0	B3
		0.0003	−31.9	0.1780	5.9	C
		0.0	—	0.1737	6.4	D
		0.0038	13.7	0.1795	2.8	E
		0.0	—	0.1682	175.0	H
		0.0213	13.2	0.1706	−175.5	I
		0.0108	14.0	0.1804	−173.9	I1
		0.0028	27.3	0.1772	6.0	J
0.10	0.0	0.0	0.0	0.1418	3.9	AN
		0.0119	−14.4	0.1464	175.4	A
		0.0139	−14.4	0.1478	175.3	B
		0.0001	−107.8	0.1344	179.9	B1
		0.0062	−13.7	0.1464	175.6	B2
		0.0003	166.6	0.1384	175.7	B3

Table 1 (*continued*)

R [m]	ϕ [Deg]	B_x[T]	θ_x [Deg]	B_y [T]	θ_y [Deg]	PROG.
		0.0006	−9.3	0.1390	4.3	C
		0.0	0.0	0.1418	3.9	D
		0.0043	13.7	0.1440	2.1	E
		0.0	—	0.1462	176.1	H
		0.0154	14.4	0.1587	179.2	I
		0.0056	13.8	0.1536	176.6	I1
		0.0003	29.5	0.1496	4.6	J
0.15	0.0	0.0	0.0	0.1185	2.1	AN
		0.0052	−14.5	0.1232	177.2	A
		0.0062	−14.3	0.1238	177.2	B
		0.0009	166.4	0.1095	177.6	B1
		0.0027	−13.7	0.1218	177.5	B2
		0.0002	166.9	0.1153	177.6	B3
		0.0008	−2.5	0.1210	2.4	C
		0.0	—	0.1185	2.0	D
		0.0024	13.6	0.1231	2.3	E
		0.0	—	0.1189	178.0	H
		0.0068	14.3	0.1268	180.0	I

Table 2
Field points on a line at 45° to the x axis

R [m]	ϕ [Deg]	B_x [T]	θ_x [Deg]	B_y [T]	θ_y [Deg]	PROG.
0.04	45.0	0.0	0.0	0.0211	−95.0	AN
		0.0003	−26.7	0.0232	−87.6	A
		0.0004	−171.8	0.0230	85.3	B
		0.0	−7.0	0.0197	−85.6	B1
		0.0001	−168.4	0.0220	−85.3	B2
		0.0	−152.7	0.0206	−85.4	B3
		0.0152	−94.8	0.0155	−94.8	C
		0.0	—	0.0212	−95.0	D
		0.0062	—	0.0224	−95.1	E
		0.0004	78.8	0.0201	−82.8	H
		0.0002	179.6	0.0230	86.2	I
		0.0001	178.0	0.0221	85.6	I1
		0.0003	83.6	0.0218	85.6	J
0.05	45.0	0.0	0.0	0.0211	−95.0	AN
		0.0006	−20.7	0.0233	−89.1	A
		0.0007	−174.1	0.0231	84.1	B
		0.0002	−0.7	0.0197	−85.9	B1
		0.0002	−174.3	0.0220	−84.8	B2
		0.0	45.4	0.0206	−85.4	B3
		0.0152	−94.8	0.0155	−94.8	C
		0.0001	−95.0	0.0212	−95.0	D
		0.0088	−95.1	0.0218	−95.1	E
		0.0004	63.9	0.0203	−82.9	H
		0.0003	178.1	0.0230	86.1	I
		0.0001	177.4	0.0220	85.6	I1
		0.0001	2.1	0.0218	85.8	J

Table 2 (*continued*)

R [m]	ϕ [Deg]	B_x [T]	θ_x [Deg]	B_y [T]	θ_y [Deg]	PROG.
0.05842	45.0	0.0091	175.2	0.0230	−71.2	AN
		0.0111	−0.3	0.0261	−115.3	A
		0.0134	2.7	0.0270	−118.4	B
		0.0098	3.4	0.0217	−111.4	B1
		0.0102	4.5	0.0245	−111.2	B2
		0.0094	4.5	0.0226	−109.9	B3
		0.0150	−94.2	0.0210	−56.6	C
		0.0106	−158.6	0.0187	−64.2	D
		0.0101	−11.5	0.0195	−64.2	E
		0.0113	177.2	0.0252	−65.0	G
		0.0094	175.8	0.0238	−70.8	G1
		0.0092	175.6	0.0233	−71.0	G2
		0.0089	6.5	0.0217	−106.6	H
		0.0119	−2.4	0.0196	127.5	I
		0.0009	−4.0	0.0241	110.0	I1
		0.0109	−3.6	0.0243	−67.4	J
0.06858	45.0	0.0783	−170.2	0.0896	−4.6	AN
		0.0782	−11.0	0.0905	−175.1	A
		0.0772	−11.4	0.0953	−176.4	B
		0.0736	−10.7	0.0830	−176.3	B1
		0.0814	−11.0	0.0943	−176.7	B2
		0.0769	−10.2	0.0874	−175.8	B3
		0.0170	−59.3	0.1230	2.3	C
		0.0752	−175.7	0.0890	9.4	D
		0.0740	−10.4	0.0920	−15.4	E
		0.0733	−169.7	0.0899	−4.5	G
		0.0805	−169.6	0.0920	−4.1	G1
		0.0790	−169.9	0.0902	−4.3	G2
		0.0736	−8.9	0.0832	−174.5	H
		0.0776	10.9	0.0868	180.0	I
		0.0807	10.6	0.0926	176.1	I1
		0.0822	10.6	0.0922	−3.7	J
0.075	45.0	0.0757	−166.8	0.1000	0.0	AN
		0.0732	−13.7	0.0969	−178.9	A
		0.0684	−13.6	0.1026	−179.9	B
		0.0696	−13.6	0.0918	179.7	B1
		0.0757	−13.7	0.1046	179.4	B2
		0.0737	−13.5	0.0972	179.7	B3
		0.0230	−33.0	0.1280	5.9	C
		0.0755	−166.3	0.1004	0.4	D
		0.0741	13.7	0.1014	4.6	E
		0.0673	−12.4	0.0971	−179.7	H
		0.0748	13.4	0.0970	179.6	I
		0.0780	13.8	0.1023	−179.7	I1
		0.0768	13.6	0.1020	0.3	J
0.10	45.0	0.0426	−166.8	0.1000	0.0	AN
		0.0517	−14.6	0.0969	−179.4	A
		0.0444	−14.3	0.1035	179.5	B
		0.0438	−13.6	0.0913	179.8	B1
		0.0432	−13.7	0.1039	179.5	B2
		0.0422	−13.5	0.0970	179.8	B3

Table 2 (*continued*)

R [m]	ϕ [Deg]	B_x [T]	θ_x [Deg]	B_y [T]	θ_y [Deg]	PROG.
		0.0425	−166.8	0.0999	0.0	D
		0.0440	13.7	0.1000	1.8	E
		0.0415	−12.4	0.0992	−179.9	H
		0.0519	14.3	0.0996	−179.6	I
		0.0458	13.8	0.1015	−179.2	I1
		0.0486	13.6	0.1011	0.1	J
0.15	45.0	0.0189	−166.8	0.1000	0.0	AN
		0.0236	−14.5	0.0993	−179.9	A
		0.0202	−14.3	0.1043	179.4	B
		0.0181	−13.6	0.0915	179.8	B1
		0.0190	−13.7	0.1032	179.6	B2
		0.0185	−13.5	0.0972	179.7	B3
		0.0580	−2.8	0.0870	2.4	C
		0.0189	−166.8	0.0999	0.0	D
		0.0186	13.7	0.0999	0.4	E
		0.0192	−12.5	0.0969	−179.6	H
		0.0258	14.3	0.0958	179.4	I
		0.0199	13.8	0.1022	−179.8	I1
		0.0201	13.6	0.1013	0.2	J

Table 3
Field points on a line at 20° to the X axis

R [m]	ϕ [Deg]	B_x [T]	θ_x [Deg]	B_y [T]	θ_y [Deg]	PROG.
0.04	20.0	0.0	0.0	0.0211	−95.0	AN
		0.0004	−6.1	0.0234	−86.3	A
		0.0004	−176.2	0.0230	−86.6	B
		0.0	−165.5	0.0197	−85.6	B1
		0.0001	−174.9	0.0220	−85.7	B2
		0.0	−81.4	0.0206	−85.4	B3
		0.0075	−94.7	0.0210	−94.8	C
		0.0	—	0.0212	−95.0	D
		0.0016	—	0.0212	−95.1	E
		0.0001	56.6	0.0197	−82.6	H
		0.0003	179.3	0.0230	86.8	I
		0.0001	178.1	0.0221	85.8	I1
0.05	20.0	0.0	0.0	0.0211	−95.0	AN
		0.0016	−0.2	0.0234	−89.9	A
		0.0002	4.5	0.0231	−90.6	B
		0.0001	−0.1	0.0197	−86.4	B1
		0.0002	−175.2	0.0220	−85.6	B2
		0.0	−162.7	0.0206	−85.4	B3
		0.0075	−94.8	0.0210	−94.8	C
		0.0001	−95.0	0.0209	−95.0	D
		0.0022	−95.1	0.0210	−95.1	E
		0.0001	−50.6	0.0197	−82.5	H
		0.0005	177.8	0.0230	86.1	I
		0.0001	177.5	0.0221	85.7	I1

Table 3 (*continued*)

R [m]	ϕ [Deg]	B_x [T]	θ_x [Deg]	B_y [T]	θ_y [Deg]	PROG.
0.05842	20.0	0.0059	175.2	0.0270	−57.3	AN
		0.0039	1.2	0.0245	−104.3	A
		0.0076	2.6	0.0359	−138.1	B
		0.0071	3.1	0.0305	−136.2	B1
		0.0064	3.9	0.0288	−126.3	B2
		0.0065	4.3	0.0273	−126.5	B3
		0.0075	−94.2	0.0278	−56.6	C
		0.0068	−158.6	0.0210	−41.5	D
		0.0026	−15.0	0.0220	−36.6	E
		0.0054	4.3	0.0244	−120.9	H
		0.0060	−2.8	0.0281	121.7	I
		0.0087	−3.8	0.0341	135.8	I1
		0.0032	−5.4	0.0247	−66.0	J
0.06858	20.0	0.0504	−170.2	0.1485	1.2	AN
		0.0047	1.1	0.0249	−106.9	A
		0.0501	−11.4	0.1531	177.1	B
		0.0468	−11.5	0.1433	176.2	B1
		0.0520	−10.8	0.1541	177.8	B2
		0.0496	−10.5	0.1464	178.0	B3
		0.0085	−59.2	0.1610	2.3	C
		0.0485	−175.7	0.1457	−4.0	D
		0.0198	−11.5	0.1606	−3.3	E
		0.0451	−8.9	0.1360	179.9	H
		0.0543	11.2	0.1448	−178.4	I
		0.0536	12.1	0.1675	−176.0	I1
		0.0049	9.4	0.1450	0.3	J
0.075	20.0	0.0486	−166.8	0.1570	4.8	AN
		0.0732	−13.9	0.1526	175.5	A
		0.0474	−13.5	0.1486	175.8	B
		0.0446	−13.7	0.1396	175.2	B1
		0.0498	−13.7	0.1606	174.8	B2
		0.0467	−13.5	0.1521	174.9	B3
		0.0112	−33.0	0.1675	5.9	C
		0.0486	−166.8	0.1589	3.4	D
		0.0446	13.7	0.1623	3.5	E
		0.0432	−12.3	0.1435	176.2	H
		0.0638	14.3	0.1662	−174.3	I
		0.0467	13.7	0.1622	−174.7	I1
		0.0483	13.8	0.1576	5.0	J
0.10	20.0	0.0274	−166.8	0.1319	3.2	AN
		0.0517	−14.4	0.1390	175.9	A
		0.0341	−14.3	0.1312	176.6	B
		0.0304	−13.6	0.1198	176.6	B1
		0.0291	−13.7	0.1352	176.4	B2
		0.0270	−13.5	0.1282	176.5	B3
		0.0208	−9.8	0.1307	4.3	C
		0.0273	−166.8	0.1319	3.2	D
		0.0268	13.8	0.1333	2.1	E
		0.0288	−12.4	0.1264	177.4	H
		0.0402	14.3	0.1312	−176.6	I
		0.0267	13.8	0.1417	−175.9	I1
		0.0230	13.6	0.1286	3.0	J

Table 3 (*continued*)

R [m]	ϕ [Deg]	B_x [T]	θ_x [Deg]	B_y [T]	θ_y [Deg]	PROG.
0.15	20.0	0.0122	−166.8	0.1142	1.7	AN
		0.0236	−14.5	0.1202	177.5	A
		0.0148	−14.3	0.1165	177.9	B
		0.0119	−13.6	0.1040	178.2	B1
		0.0127	−13.7	0.1169	178.0	B2
		0.0117	−13.5	0.1109	178.1	B3
		0.0291	−2.8	0.1144	2.4	C
		0.0121	−166.8	0.1141	1.7	D
		0.0133	13.7	0.1138	1.7	E
		0.0135	−12.4	0.1097	178.9	H
		0.0170	14.3	0.1165	−177.9	I
		0.0120	13.8	0.1191	−177.8	I1
		0.0134	13.6	0.1178	2.1	J

Table 4
Comparison of global quantities

	Time average	Amplitude	Phase (Deg)	PROG.
	0.0	10569.0	12.4	AN
Total eddy	0.0	11385.5	166.4	A
current in	0.0	11239.0	166.5	B
1/4 region	0.0	9664.0	167.2	B1
[A]	0.0	10933.0	167.1	B2
	0.0	10270.0	167.2	B3
	—	10325.0		D
	—	10511.0	—	E
	—	10923.0	13.1	G
	—	10851.0	12.8	G1
	—	10648.0	12.6	G2
	0.0	9819.0	169.1	H
	0.0	11300.0	−166.4	I
	0.0	10978.0	−167.0	I1
	0.0	10730.0	14.28	J
	2288.2	2043.0	27.6	AN
Power loss	2688.0	2412.7	−30.1	A
in 1/4	2613.0	2346.0	−29.6	B
region	1933.0	1729.0	−28.4	B1
[Watt/m]	2454.0	2194.0	−28.6	B2
	2166.0	1935.0	−28.3	B3
	20578.0	—	—	C
	2177.0	1949.0	27.0	D
	—	1912.4	—	E
	2445.0	2202.7	28.7	G
	2411.7	2158.1	28.4	G1
	2322.0	2078.0	27.0	G2
	2012.0	1771.0	−24.5	H
	2616.1	2360.1	29.6	I
	2467.4	2210.0	28.7	I1
	2389.0	—	—	J
	1.60	1.41	−8.8	AN
Stored	1.735	1.54	7.1	A
energy in	1.69	1.49	7.5	B
1/4 region	1.37	1.21	7.5	B1

Table 4 (*continued*)

	Time average	Amplitude	Phase (Deg)	PROG.
	1.67	1.48	8.0	B2
$0.05717 < r <$	1.52	1.39	7.9	B3
0.06985	0.04	—	—	C
[Joule/m]	1.92	1.20	−27.7	D
	—	1.25	—	E
	1.6735	1.48	−8.0	G
	1.6749	1.482	−8.1	G1
	1.6128	1.4271	−8.6	G2
	1.42	1.26	8.8	H
	0.00	3.13	119.6	I*
	0.00	2.93	118.7	I1*
	1.75	1.54	−7.1	I**
	1.6975	1.50	−7.8	I1**
	1.629	—	—	J
	0.228	0.228	170.0	AN
Stored	0.275	0.270	−176.6	A
energy in	0.270	0.260	−175.8	B
1/4 region	0.2	0.19	−171.8	B1
	0.25	0.25	−171.9	B2
$r < 0.05715$	0.22	0.22	−170.8	B3
[Joule/m]	2.130	—	—	C
	0.229	0.229	169.9	D
	—	0.230	—	E
	0.25023	0.25023	171.2	G
	0.2418	0.2418	170.8	G1
	0.2323	0.2328	170.3	G2
	0.202	0.202	−165.9	H
	0.268	0.268	172.7	I
	0.2475	0.2475	171.3	I1
	0.2406	—	—	J
	273.6	273.1	0.5	AN
Stored	363.0	362.2	−1.0	A
energy in	265.0	264.0	−1.3	B
1/4 region	232.0	232.0	−1.1	B1
	277.0	276.0	−1.2	B2
$r > 0.06985$	261.0	260.0	−1.1	B3
[Joule/m]	2365.0	—	—	C
	273.5	273.8	0.6	D
	—	286.2	—	E
	283.6	282.5	1.2	G
	286.1	285.4	1.2	G1
	259.0	258.0	0.1	H
	284.1	283.4	1.28	I
	286.3	285.6	1.2	I1
	361.8	—	—	J
Stored	—	11.0	—	A
energy of	12.3	10.9	−1.2	B
induced	9.2	8.1	−1.1	B1
field in	12.8	11.4	−1.2	B2
1/4 region	11.3	10.1	−1.1	B3
	0.0	2.6	117.0	D
	—	2.8	—	E

Table 4 (*continued*)

	Time average	Amplitude	Phase (Deg)	PROG.
	−294.0	305.0	174.9	H
	13.7	13.6	27.1	I
	13.4	13.3	26.0	I_1
	−333.4	351.6	−173.6	AN
Force on	−385.9	407.0	171.5	A
1/4 region	−375.0	396.0	172.0	B
[N/m]	287.0	302.0	172.6	B1
	−356.0	376.0	172.6	B2
Fx	−287.0	302.0	172.6	B3
	−314.0	348.0	−175.0	D
	—	−343.7	—	E
	−353.7	375.0	−173.0	G
	−350.8	370.5	−173.0	G1
	−337.8	356.7	−173.5	G2
	−294.0	305.0	174.9	H
	−390.1	393.5	−172.5	I
	−373.5	376.4	−172.8	I1
	345.1	—	—	J
	−166.7	165.7	−155.8	AN
Force on	−196.0	375.0	163.1	A
1/4 region	−190.0	363.0	163.6	B
[N/m]	−143.0	274.0	164.7	B1
	−179.0	343.0	164.6	B2
Fy	−143.0	274.0	164.0	B3
	−157.0	164.0	−158.0	D
	—	155.7	—	E
	−178.4	177.7	−154.8	G
	−175.8	174.8	−155.1	G1
	−169.3	168.3	−155.6	G2
	−146.0	143.0	157.4	H
	−169.6	188.7	−154.0	I
	−161.2	178.2	−154.8	I1
	172.1	—	—	J

Key to programs.
AN—Analytical Solution, Oskar Biro, Technical University, Budapest.
A —PE2D, Chris Emson, Rutherford Laboratory.
B —PE2D, Robert Lari, Argonne National Laboratory.
B1 —PE2D, Robert Lari, Same as B but with Quadratic Triangular Elements.
B2 —PE2D, Robert Lari, 4 times the number of elements in B.
B3 —PE2D, Robert Lari, 4 times the number of elements in B1.
C —PROFI, Technische Hochschule, Darmstadt.
D —No Name, Toshiya Morisue, Tokushima University.
E —EDDYNDT, Nathan Ida, The University of Akron.
G —ANSYS, Dale Ostergaard, Swanson Analysis Systems, Inc.
G1 —ANSYS, Dale Ostergaard, 4 times the number of elements in G.
G2 —ANSYS, Dale Ostergaard, 4 times the number of elements in G with modified boundary (outer boundary at 0.84 m).
H —No name, E.M. Deeley, King's College, London.
I —FIELD/A2JW, T. Nakata, Okayama University.
I1 —Same as I but with four times the number of elements.
J —WEMAP, V.K. Garg, Westinghouse Electric Corporation.
* —Method A (see [16]).
** —Method B (see [16]).

are shown to indicate the difficulty most codes had in calculating values close to the center.

The results presented are also summarized in Figs. 3–5. In all cases, the lowest and highest results reported are presented together with the analytical solution for the X and Y components of the flux density. In most cases, the results are quite similar, but at times the variations are relatively large, especially within and close to

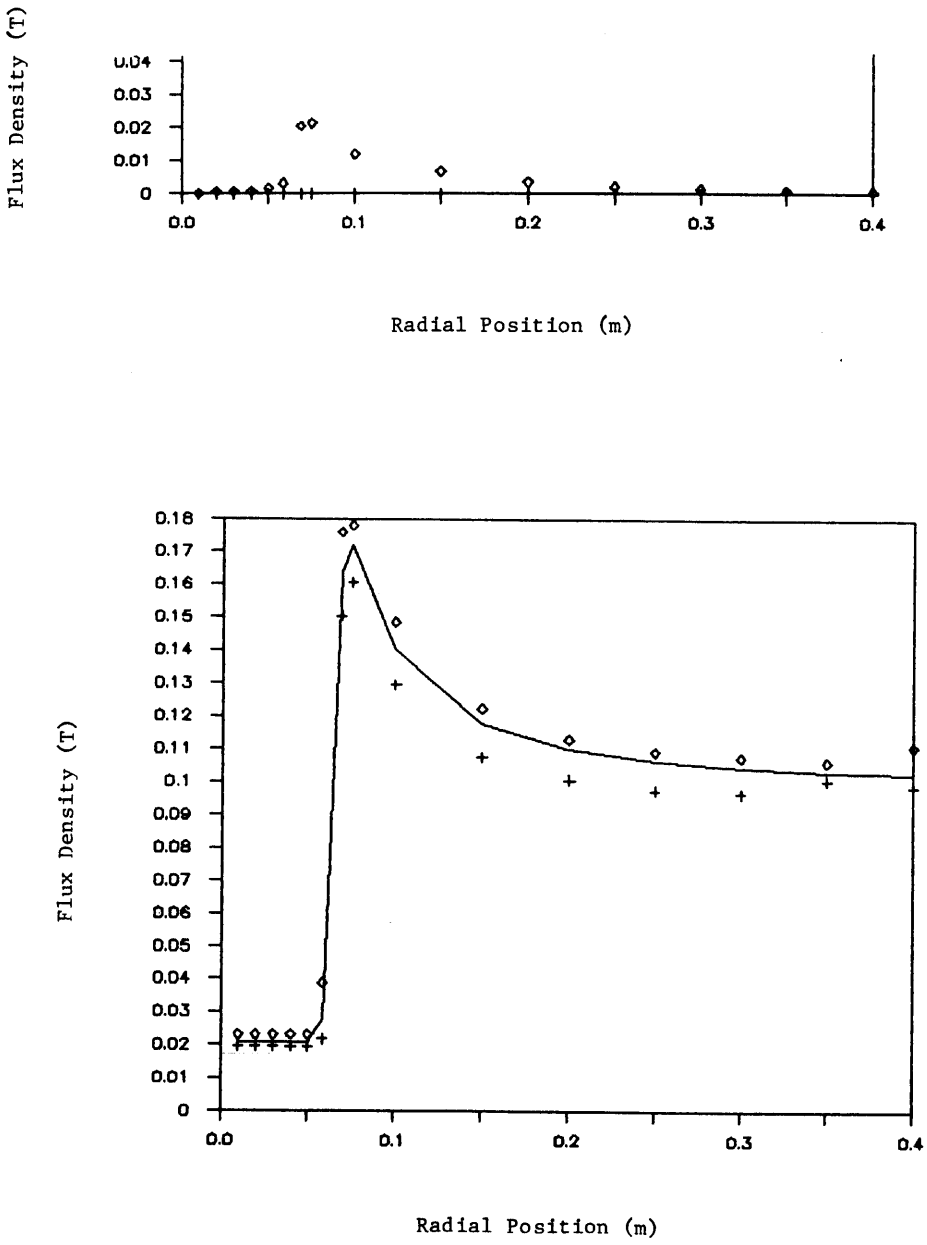

Figure 3: Flux density versus position at 0.0°. (a) B_x; (b) B_y. ◇ Maximum calculated result; — Analytic solution; + Minimum calculated result.

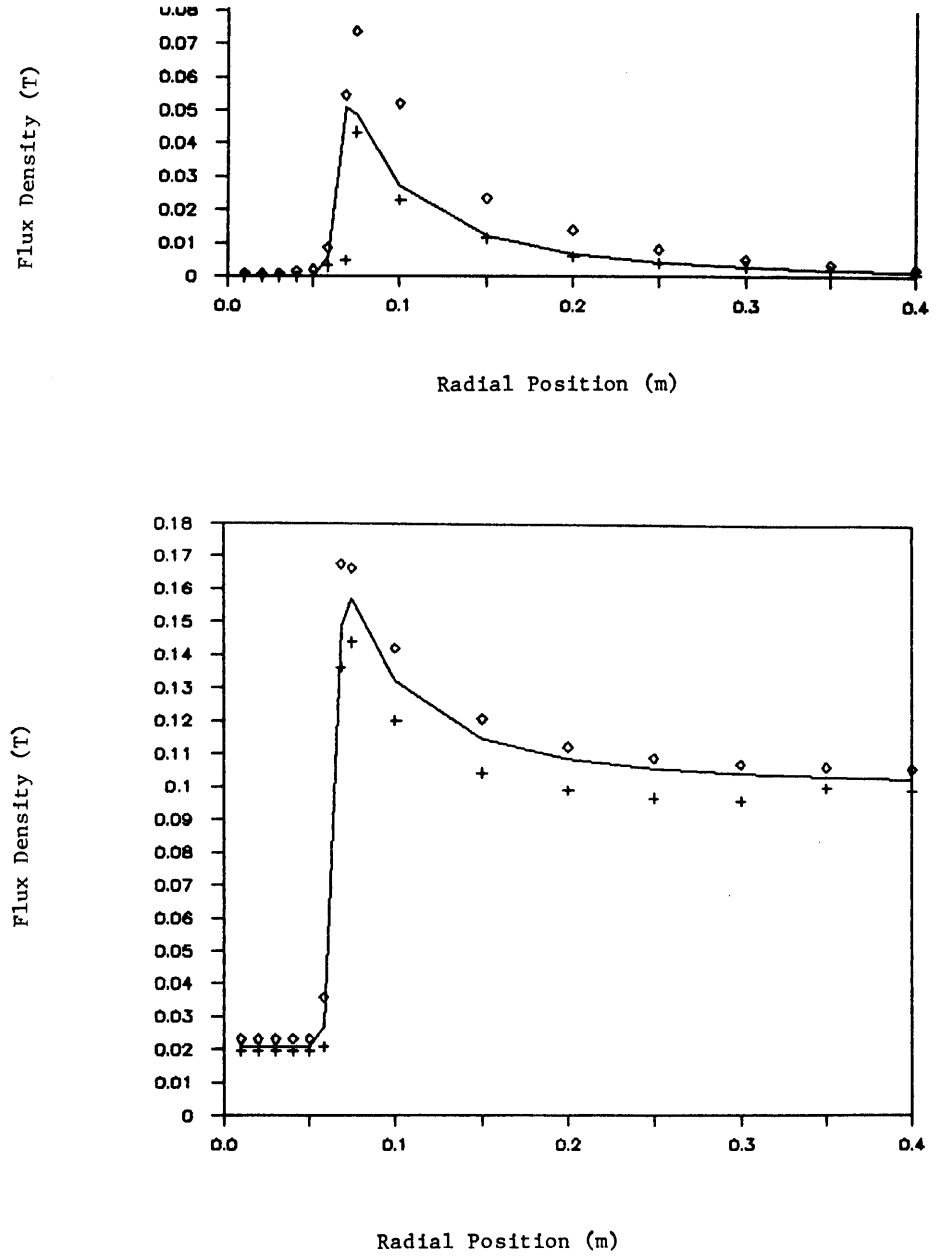

Figure 4: Flux density versus position at 7.5°. (a) B_x; (b) B_y. ◇ Maximum calculated result; — Analytic solution; + Minimum calculated result.

the cylinder. At these points the variation can be upward of 30% while inside and outside the cylinder they are normally below 10%. In particular, Fig. 3 shows that while the analytic result for the X component of the flux density on the X axis should be zero, most computed results are not. As with the tables, the figures only present representative results out of the available data. Complete results can be found in

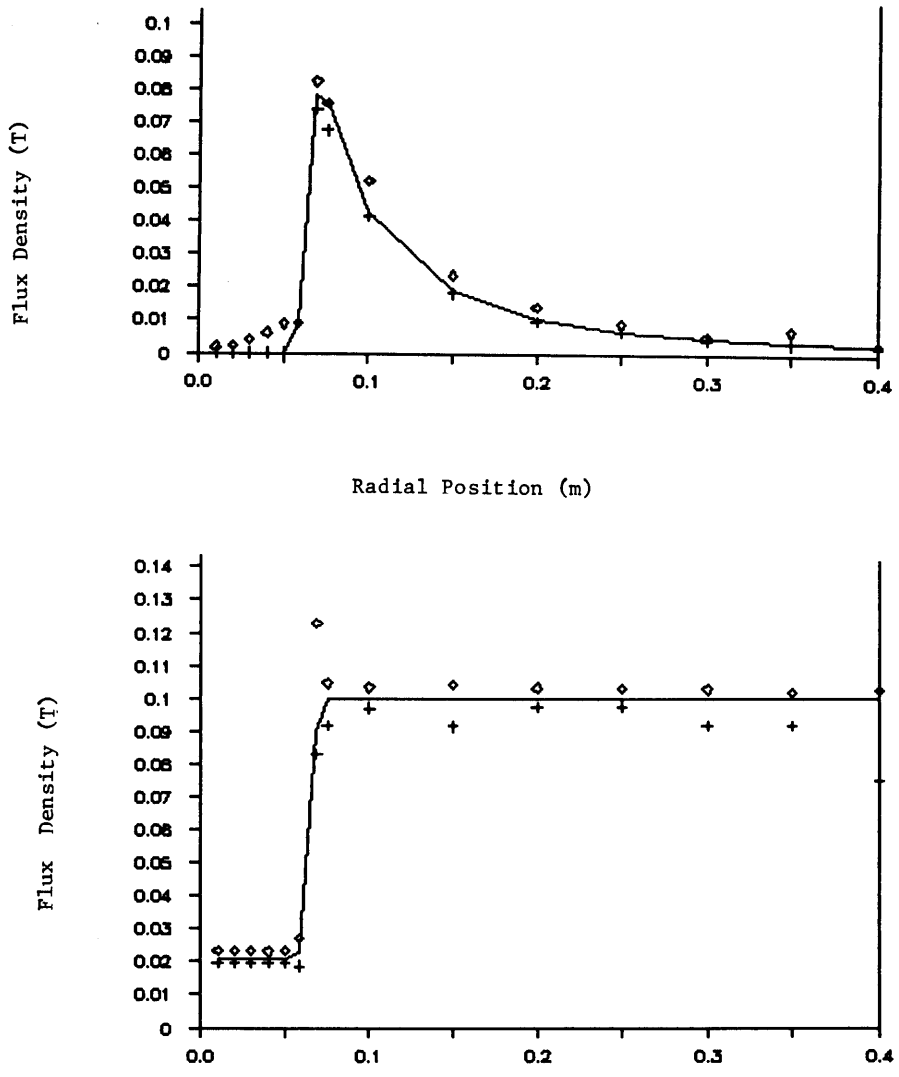

Figure 5: Flux density versus position at 14.0°. (a) B_x; (b) B_y. ◇ Maximum calculated result; — Analytic solution; + Minimum calculated result.

individual contributions listed in the references and in the proceedings of the Graz workshop.

REFERENCES

[1] International Electromagnetic Workshop: Test Problems, April 1986 (available from Larry Turner, Argonne National Laboratory).

[2] L.R. Turner, K. Davey, C.R.I. Emson, K. Miya, T. Nakata and A. Nicolas, Problems and workshops for eddy current code comparison, presented at COMPUMAG '87, Graz, Austria, 1987.
[3] R.J. Lari and L.R. Turner, Survey of eddy current programs, IEEE Trans. Magn. MAG-19(6) (1983) 2474–2481.
[4] L.R. Turner, G.R. Gunderson, M.J. Knott, D.G. McGee, W.F. Praeg and R.B. Wehrle, Results from the Felix experiments on electromagnetic effects in hollow cylinders, IEEE Trans. Magn. MAG-21(6) (1985) 2324–2328.
[5] C. Emson, Proceedings of the Regional Electromagnetic Workshop at Argonne National Laboratory, ANL/FPP/TM-210, pp. 69–73, June 1986.
[6] R.J. Lari and L. Turner, Calculation of test problem 2 for the International Electromagnetic Workshop, Proc. Int. Electromagnetic Workshop, Rutherford Appleton Laboratory, RAL-86-049, pp. 69–75, March 1986.
[7] R.J. Lari, Recalculation of test problem 2 for the International Electromagnetic Workshop, Proc. Regional Electromagnetic Workshop at Argonne National Laboratory, ANL/FPP/TM-210, pp. 47–61, June 1986.
[8] U. Hamm, Solution of test problem 2, infinitely long cylinder in sinusoidal field using PROFI, Proc. Int. Electromagnetic Workshop, Rutherford Appleton Laboratory, RAL-86-049, pp. 51–68, March 1986.
[9] T. Morisue, Problem 2: Infinitely long cylinder in a sinusoidal field, Proc. Regional Electromagnetic Workshop at Argonne National Laboratory, ANL/FPP/TM-210, pp. 38–46, June 1986.
[10] N. Ida, Infinitely long cylinder in a sinuosoidal field, Proc. Regional Electromagnetic Workshop at Argonne National Laboratory, ANL/FPP/TM-210, pp. 62–68, June 1986.
[11] A. Ivanyi, I. Bardi and O. Biro, Analytical solution to problem 2 of the International Electromagnetic Workshop, Proc. Int. Electromagnetic Workshop, Rutherford Appleton Laboratory, RAL-86-049, pp. 39–49, March 1986.
[12] D.F. Ostergaard, Infinitely long cylinder in a sinusoidal field, presented at the International Workshop for Eddy Current Code Comparison, Graz, 1987.
[13] P.C. Kohnke, ANSYS Theoretical Manual, Swanson Analysis Systems, Inc., Houston, PA., 1987.
[14] E.M. Deeley, Improved surface impedance methods, presented at COMPUMAG, '87, Graz, Austria, 1987.
[15] E.M. Deeley, Infinitely long cylinder in a sinusoidal field, presented at the International Workshop for Eddy Current Code Comparison, Graz, 1987.
[16] T. Nakata, N. Takahashi, K. Fujiwara and K. Okazaki, Calculation of infinitely long cylinder (Problem 2), Proc. Int. Workshop for Eddy Current Code Comparison, Tokyo, 1986.
[17] V.K. Garg, M. Ashkin and D. Simmen, WEMAP solution of problem 2, presented at the International Workshop for Eddy Current Code Comparison, Graz, 1987.